MONITORING CRACK GROWTH IN A DCB TEST USING A SURFACE-BONDED CHIRPED FBG SENSOR

A.R.Sanderson[1*], S.L.Ogin[1], A.D.Crocombe[1], M.R.L Gower[2], R.J. Lee[3], S. C. Tjin[4], B. Lin[4]
[1]Faculty of Engineering and Physical Sciences, University of Surrey, Guildford, United Kingdom.
[2]National Physical Laboratory, Teddington, United Kingdom [3]ESR Technology Ltd, Abingdon, United Kingdom, [4]School of Electrical and Electronic Engineering, Photonics Research Centre, Nanyang Technological University, Singapore
*A.R.Sanderson (A.R.Sanderson@surrey.ac.uk)

Keywords: *DCB, chirped FBG, delamination growth, monitoring*

Abstract

Delamination growth within transparent, unidirectionally reinforced glass fibre/epoxy double-cantilever beam (DCB) specimens has been monitored using a surface-mounted chirped fibre Bragg grating (CFBG) sensor. The specimens were tested using a constant displacement rate, with the delamination length being measured using (i) surface-mounted CFBG sensors, (ii) *in situ* photography, and (iii) surface-mounted strain gauges. The DCB specimens showed characteristics typical of such material, with the development of extensive fibre bridging and pronounced R-curve behaviour. A distinct perturbation in the reflected spectra, when monitoring the delamination growth using the CFBG sensors, was indicative of the location of the delamination front during the test. The *in situ* photographs and the surface strain measurements provided by the strain gauges were used to predict the experimentally determined CFBG reflected spectra, with good agreement between prediction and experiment. These results enabled the delamination length to be measured using the CFBG sensor technique to within 4 mm over the 60 mm sensor length.

1. Introduction

With the expanding use of large composite structures, such as wind turbine blades, the monitoring of delamination growth is an area of increasing interest. There is a need to determine both whether a delamination has initiated, and also the current location of the damage, and/or its growth rate. Various NDE (non-destructive evaluation) techniques are potentially able to detect the location of delaminations, including acoustic emission, electric resistance measurements, shearography and thermography [1-4]. It is, however, likely to be difficult to employ many of the currently proposed techniques either due to the physical difficulties of implementation (e.g. complications arising out of the connections required), or the unproven nature of the technique. The ability to be able to embed fibre optic sensors within a composite structure, and the proven usage of fibre optical sensors for monitoring large structures [e.g. 5] make these sensors important candidates.

Chirped FBG (CFBG) sensors embedded within composite materials have been shown to be able to monitor delamination growth in simple lap-joints [6-8], where the changes in the reflected spectra from such sensors are generally easier to interpret than for uniform FBG sensors.

The relative ease of interpretation of CFBG reflected spectra with regard to damage development is a result of the relationship between the spectral bandwidth of the reflected spectrum (typically 20 nm) and the sensor length (typically 60 mm). If the sensor is embedded in a composite material subjected to a tensile uniform strain, all the grating spacings are increased and the entire spectrum shifts to higher wavelengths – just as for a uniform FBG. However, if the strain field is perturbed by damage in the composite, so that the smooth linear increase in the grating spacing is disrupted, then a perturbation appears in the reflected spectrum that can be used to monitor the physical location of the damage.

The previous use of *embedded* CFBG sensors to monitor the progression of a delamination has been extended here to the use of *surface-bonded* sensors. It is important to determine whether a surface-bonded sensor can also monitor delamination growth, as in many situations, it will be impractical to embed sensors within a structure.

2. Experimental methods

2.1 Materials

A transparent unidirectional GFRP laminate was manufactured using a frame-winding technique described in detail elsewhere [e.g. 7], consisting of E-glass fibres ($V_f \approx 0.6$) in a Shell Epikote 828 epoxy resin matrix. The nominal dimensions of the specimens were 150 mm x 25 mm x 5 mm, and a 40 mm long nylon film (with a thickness of 50 μm), spanning the entire width of the specimen at the centre line (see figure 1a) was included to initiate the delamination. On both the upper and lower surfaces of the specimen at one end, aluminium brackets were bonded using DP-490 adhesive to enable the specimen to be loaded in the testing machine. A 60 mm section of each specimen was instrumented on one surface, beyond the position of the end of the 40 mm nylon insert, with strain gauges and a CFBG sensor. At the centre-line of one half of the DCB specimens, six 1 mm gauge length strain gauges (type: N11-FA-1-120-23) with a nominal spacing of 10 mm were bonded, with the first gauge located 5 mm from the end of the insert. On the adjacent half-strip of the specimen, a 60 mm CFBG sensor (manufactured by TeraXion) was bonded to the surface of the specimen, parallel to the length of the specimen and the strain gauges, using M-Bond 610 adhesive. The CFBG sensor had a full width at the half-maximum of the reflected spectrum of 20 nm, and a centre wavelength of 1550 nm.
The strain gauges were connected to a multi-channel data logger (Solitron Orion 3503) which enabled the six strain gauges to be logged simultaneously. The optical fibre sensor was connected to a Smart Fibres W-4 laser interrogator [9].

2.2 Method

The DCB specimens were loaded quasi-statically using a computer-controlled servo-hydraulic testing machine (Instron 4505) at a constant opening displacement rate of 1 mm/min. The strain gauge data and the CFBG spectra were logged automatically every 2 seconds and 60 seconds, respectively. A USB camera was used to photograph the specimens in transmitted light every 60 seconds, with the specimens viewed from the face opposite to the instrumented face. After the delamination had propagated beyond the 60 mm sensor region, the test was stopped, at which point the opening displacement at the loading line was about 35 mm.

3. Results and discussion

3.1 R-curve behaviour and strain gauge results

The delamination initiated from the nylon film during testing, and propagated along the specimen with increasing displacement of the DCB arms (note that all delamination lengths, unless otherwise indicated, are measured from the end of the nylon insert, so that 40 mm needs to be added to these values to obtain the total delamination length). The delamination front position can be readily determined from the *in situ* photographs (further details are given in [10]), due to the transparency of the specimens. The delamination lengths were measured along the centre-line of the specimen; there is a slight curvature of the delamination front so that the lengths which would be measured at the edges of the specimens would be up to approximately 2.5 mm longer.
The load-displacement curves for the DCB tests enabled the toughness to be determined and the R-curve behaviour, delamination initiation value (about 200 J/m^2) and plateau propagation value (about 800 J/m^2) found are typical of these specimens [11]. As is well-known, the development of an R-curve in these materials is related to fibre bridging. In this work, the development of fibre bridging is important in modelling the reflected CFBG spectra since, as will be seen below, the crack closing forces alter the curvature of the arms of the DCB specimen. The R-curve showed that fibre bridging was not fully developed until total delamination lengths of about 75 mm, and this is reflected in the measurements of the surface strains recorded by the surface-mounted strain gauges.
Figure 2 shows an example of the compressive strain changes measured by each of the six strain gauges as a function of the delamination length (measured at the centre of the specimen). The inset figure shows the strain gauge numbering system, where strain gauge 1 (SG1) is the strain gauge located 5 mm from the end of the insert. The six vertical lines included in the figure indicate the actual position of the centre

of each strain gauge (nominally 10 mm apart) with respect to the delamination length. For example, the line which represents the location of SG2 is at 14 mm.
The strain gauge results from these experiments are similar to the strain data derived by Stutz et al [12] from their multiplexed FBGs embedded close to the mid-plane of a unidirectionally reinforced CFRP laminate tested as a DCB specimen. As found by Stutz and colleagues, the presence of the fibre bridging complicates the strain changes. The prediction of the CFBG reflected spectra, including such complications, are described in the next section.

3.2 CFBG sensor results for the DCB tests

Figure 3 shows typical changes in the reflected spectra of a surface-bonded CFBG sensor for increasing delamination lengths. The sensor was oriented so that the low wavelength end of the sensor was near to the nylon insert and all delamination lengths are quoted here as additional to the 40 mm insert length.
The reflected spectra (i) before delamination growth, and (ii) after the delamination has grown 20 mm, are shown in figure 3(a). There are two noticeable changes in the reflected spectra as a consequence of delamination growth. The first is the development of a perturbation in the spectrum (i.e. an extended dip in intensity) with a minimum at approximately 1543 nm. The second is the shift of the low wavelength end of the reflected spectrum to lower wavelengths, as indicated by the arrow in the figure. The CFBG sensor is bonded to the specimen surface and there is a rapidly increasing compressive strain experienced by the sensor as the position of the delamination front approaches. As a consequence, the grating spacings are increasingly compressed up to the position of the delamination front. Behind the delamination front, although the compressive strains remain high, the strain gradient decreases. High strain gradients cause significant perturbations in the reflected spectra of CFBG sensors (uniform strains just shift the spectra to higher or lower wavelengths, depending on the sign of the strain). Consequently, the dip in intensity corresponds with the approximate location of the delamination front, which can be tracked by monitoring the movement of the perturbation.
The perturbation in the spectrum moves to higher wavelengths as the delamination grows, as shown in figures 3(b) and 3(c), since the high strain gradients are associated with the current position of the delamination front. Additionally, the low-wavelength end of the spectrum moves to slightly higher reflected wavelengths because the curvature of the DCB arm relaxes as the delamination front progresses to greater distances from the physical location of the low-wavelength end of the CFBG sensor. Similarly, as the delamination front nears the position of the high-wavelength end of the sensor, such as with the delamination length of 57.1 mm (figure 3c), the spectrum shows the movement of the high-wavelength end of the reflected spectrum to lower wavelengths due to the compressive strains associated with the delamination.
In summary, the perturbation in the reflected spectrum is a measure of the current location of the delamination. However, in order to be able to track the position of the delamination with precision, it is important to be able to predict the reflected spectrum and to locate the delamination front position within the spectrum. As described in the next section, this is accomplished with the surface strain observations provided by the surface-mounted strain gauges, together with the *in situ* photographs of delamination growth.

4. Prediction of the CFBG reflected spectrum

For CFBG sensors which are used to monitor the initiation and propagation of damage in composite materials, the prediction of changes to the reflected spectra can normally be achieved using a finite-element analysis of the composite under load containing the damage and a commercially available programme for predicting reflected spectra incorporating strain distributions (OptiGrating; [13]). In the present work, the strain distribution needs to take account of the development of fibre bridging in the DCB specimens. It has been shown by Stutz et al [12] that a semi-empirical method, based on a finite-element model employing cohesive zone elements, can be used successfully to model the effect of fibre bridging. In the current work, however, additional data for the strain distribution is available in the form of the independently-obtained surface strain measurements (from the surface-bonded strain gauges). Consequently, these strain gauge measurements can be used for the prediction, and interpretation, of the CFBG reflected spectra.
A strain profile for the variation in the surface compressive strains as a function of distance in the vicinity of a delamination is shown in figure 4, where the delamination front is located in this figure at 0 mm on the x-axis. This plot was constructed from the strain gauge data shown in figure 2 by

plotting the strain variation for a specific strain gauge (SG4) as the delamination grew adjacent to the gauge. It is possible to position the strain distribution accurately, with the aid of the strain gauge and photographic data, as if the delamination was located at exactly the mid-point of the CFBG sensor i.e. for a delamination length of 30 mm. This strain distribution is therefore relevant to total delamination lengths greater than 70 mm, by which point fibre bridging in these specimens has developed fully. The resolution in experimental strain gauge data was not sufficient to allow for the direct use of the data recorded by the data-logger. Therefore, a smooth curve was fitted to the data (as shown in figure 4), from which the reflected spectrum was predicted. The optical parameters used in the prediction were uniform apodization, Poisson's ratio of 0.16 and photo-elastic coefficients $p_{11} = 0.113$ and $p_{12} = 0.252$, with an index modulation, Δn, of 0.000219 [7].

A comparison of an experimentally-recorded reflected spectrum and the predicted spectrum for the same delamination length are shown in figures 5(a) and (b). Figure 5(a) shows an experimentally determined reflected spectrum from a specimen when the delamination length was 30 mm ± 1 mm along the 60 mm sensor, where the uncertainty arises from locating the delamination front position from the photographs. The predicted spectrum for a delamination which is exactly 30 mm in length, using the strain distribution shown in figure 4, is shown in figure 5(b). It can be seen that there is good agreement between the experimentally determined and predicted reflected spectra. This prediction has been used to derive the delamination lengths for all of the spectra recorded in the tests. Within the predicted spectrum of figure 5(b), the feature in the perturbation which corresponds to the delamination length of 30 mm is the minimum in the perturbation. Consequently, it has been assumed that, for each spectrum, the delamination front position corresponds to the location of the minimum in the perturbation. The delamination length has been calculated using the difference in wavelength between the low-wavelength end of the spectrum and the position of the minimum in the perturbation, as a fraction of the full-width at half-maximum of the spectrum. This fraction is then converted to a length, assuming linearity between the spectral bandwidth and the physical length of the sensor (60 mm).

The CFBG sensor measurements of delamination length plotted against the photographically measured delamination length for three DCB specimens are shown in figure 6. The results show that the delamination lengths measured using the CFBG sensor in this way are within about 4 mm of the photographically measured delamination lengths, over the entire 60 mm length of the CFBG sensor. Consequently, the results demonstrate that a surface-bonded CFBG sensor has the potential to monitor delamination lengths within a composite structure. It should be highlighted that the accuracy with which the delamination length can be measured will be a function of the geometry of the structure and the material. For example, for the present geometry, thicker DCB arms will reduce the accuracy of the measurements.

4. Concluding remarks

The growth of delaminations in DCB specimens fabricated from transparent, unidirectionally reinforced glass fibre/epoxy has been monitored using surface-bonded CFBG sensors and strain gauges, together with *in situ* photography. Changes in the surface strains with delamination growth have been identified and understood, and interpretation of the CFBG reflected spectra has been achieved with the help of measurements of surface strain changes, using strain gauges. A perturbation in the CFBG reflected spectra, consisting of a dip in the reflected intensity, indicated the presence of the delamination front, since the perturbation was associated with high surface strain gradients in the vicinity of the delamination front. Good agreement was obtained between the predicted CFBG reflected spectra and the experimentally measured reflected spectra, using the independently obtained surface strain measurements from the strain gauges for the predictions. This enabled the position of the growing delamination to be determined using the CFBG sensor to within about 4 mm of its photographically determined position.

Figures

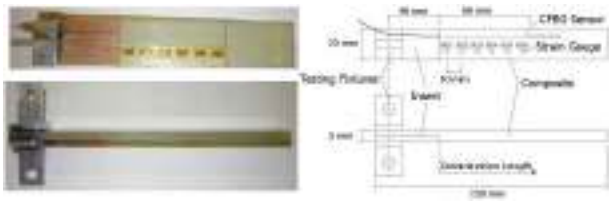

(a) (b)

Fig. 1 – (a) Images of a specimen, showing the same views; (b) Schematic diagram showing plan (above) and edge (below) views of a specimen

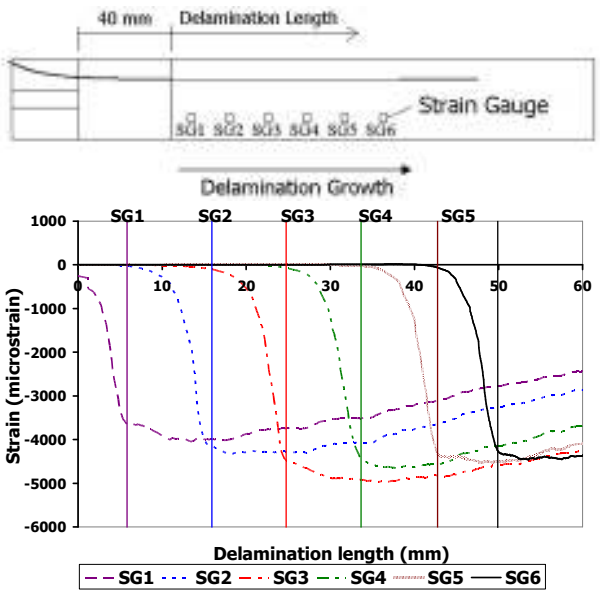

Fig. 2 - A typical plot of strain measured by surface mounted strain gauges (SG1 to SG6) against delamination length.

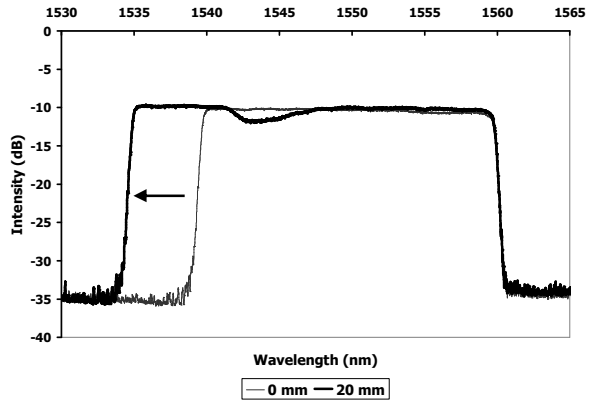

(a)

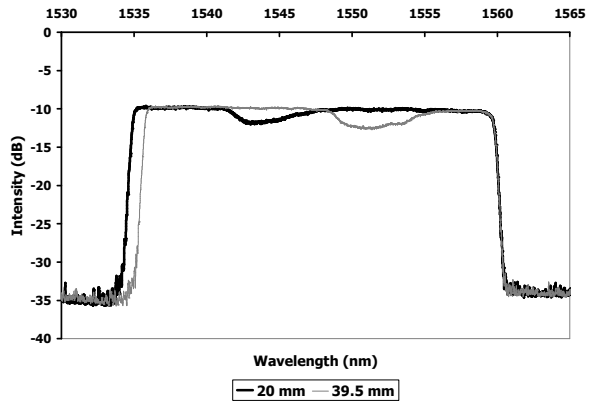

(b)

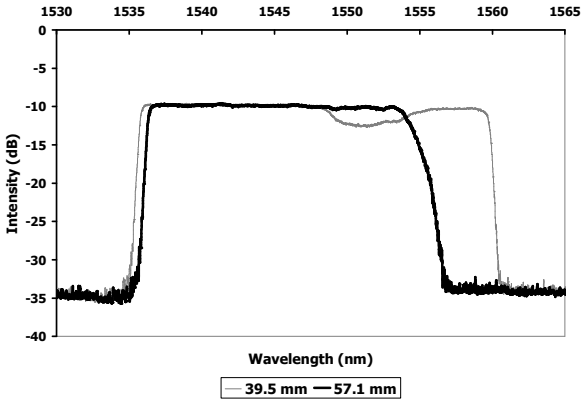

(c)

Fig. 3 - The reflected spectra from a specimen with delamination lengths of (a) 0 mm and 20 mm; (b) 20 mm and 39.5 mm; (c) 39 mm and 57.1 mm.

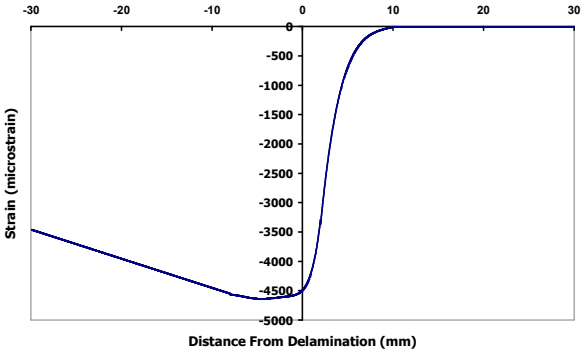

Fig. 4 - Strain distribution, derived using the surface-mounted strain gauges, for a delamination that is 30 mm in length.

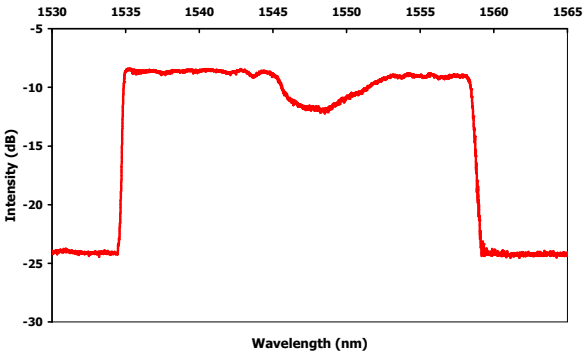

(a)

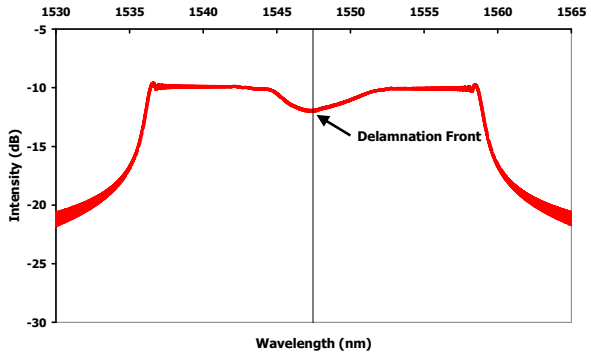

(b)

Fig. 5 - (a) The experimentally-determined reflected spectrum for a delamination which is half-way along the 60 mm sensor (± 1 mm) (b) predicted spectrum for a delamination which is exactly half-way along the 60 mm sensor region.

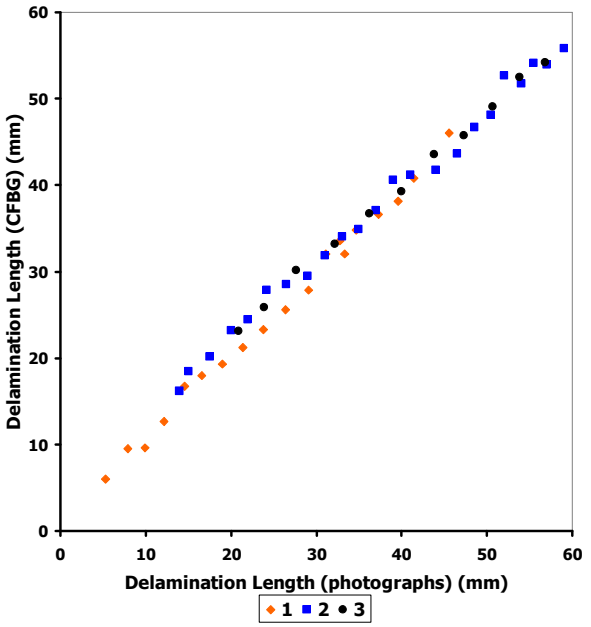

Fig. 6 - A plot of the CFBG determined delamination lengths plotted against the photographically determined delamination lengths.

References

[1] Z. Wei, L.H. Yam , L. Cheng "Detection of internal delamination in multi-layer composites using wavelet packets combined with modal parameter analysis". *Composite Structures* No. 64, pp. 377-387, 2004.

[2] A. Todoroki, Y. Tanaka "Delamination identification of cross-ply graphite/epoxy composite beams using electric resistance change method". *Composites Science and Technology* No. 62, pp. 629-639, 2002.

[3] I. Amenabar, A. Mendikute, A. López-Arraiza , M. Lizaranzu, J. Aurrekoetxea "Comparison and analysis of non-destructive testing techniques suitable for delamination inspection in wind turbine blades". *Composites: Part B*, IN Press, DOI: 10.1016/j.compositesb.2011.01.025, 2011.

[4] R. Raišutis, E. Jasiūnienė, R. Šliteris, A. Vladišauskas"The review of non-destructive testing techniques suitable for inspection of the wind turbine blades". *ULTRAGARSAS Journal*, No. 63, pp. 26-30, 2008.

[5] Y.M. Gebremichael, W. Li, W.J.O. Boyle, B.T. Meggitt, K.T.V. Grattan, B. McKinley, G.F. Fernando, G. Kister, D. Winter, L. Canning, S. Luke "Integration and assessment of fibre Bragg grating sensors in an all-fibre reinforced polymer composite road bridge". *Sensors and Actuators*; *A118*, pp. 78-85, 2005.

[6] J. Palaniappan, S.L. Ogin, A.M. Thorne, G.T. Reed, A.D. Crocombe, T.F. Capell, S.C. Tjin, L. Mohanty "Disbond growth detection in composite–composite single-lap joints using chirped FBG sensors". *Composites Science and Technology*, No. 68, pp. 2410-2417, 2008.

[7] J. Palaniappan, H. Wang, S.L. Ogin, A. Thorne, G.T. Reed, S.C. Tjin, L.N. McCartney "Prediction of the reflected spectra from chirped fibre Bragg gratings embedded within cracked cross-ply laminates". *Measurement Science and Technology*, No. 17, pp. 1609-1614, 2006.

[8] S. Takeda, Y. Okabe, N. Takeda "Monitoring of Delamination Growth in CFRP Laminates using Chirped FBG Sensors". *Journal of Intelligent Material Systems and Structures*, No. 19, pp. 437-444, 2008.

[9] Smart Fibres Ltd. W4 Laser Interrogator: User guide and Smartsoft interface instructions.

[10] A.R. Sanderson, S.L. Ogin, A.D. Crocombe, M.R.L. Gower, R.J. Lee "Use of a surface-mounted chirped fibre bragg grating sensor to monitor delamination growth in a double-cantilever beam test"; submitted to *Composites Science and Technology*

[11] J.J. Lee, S.L. Ogin, P.A. Smith "Interlaminar fracture toughness of glass fibre laminates additionally reinforced with carbon beads". *Fifth Symposium on Composite Materials: Fatigue and Fracture*, ASTM, Atlanta, Georgia, May 1993; published as ASTM STP 1230, R H Martin, Ed, pp38-60, 1995

[12] S. Stutz, J. Cugnoni, J. Botsis "Studies of mode I delamination in monotonic and fatigue loading using FBG wavelength multiplexing and numerical analysis". *Composites Science and* Technology, No. 71, pp. 443-449, 2011.

[13] OptiGrating, Integrated and Fibre Optical Gratings Design Software (version 4.2), Optiwave Corporation, Canada.